



## **PORE-LEVEL CFD INVESTIGATION OF THE PERMEABILITY AND FORM DRAG OF "STRUCTURAL - ADAPTED" POROUS METALS.**

**SAMUEL, MATHEW BASHARO, ENGR. DR. A. J. OTARU.**

*Department of Chemical Engineering, Federal University of  
Technolog, Minna, Nigeria.*

### **ABSTRACT**

*The transport of fluid in porous metallic structures is of considerable interest due to their unique and combined. Characteristics of high surface area and large pore volume, enabling their suitability as energy and impact loading material. This work present a combined utilization of image processing and pore-level computational fluid dynamics modelling and simulation of fluid flow across "real" and geometrically - adapted commercial foams. Pore-structure related and flow properties of the porous structure were obtained using the combined techniques with reasonable correlation of experimentally derived values. The modelling approach used herein could assist in the design of efficient porous metal foams for fluid transport application.*

**Keywords:** *Metal foam. CFD. Pore-level. Permeability.*

### **INTRODUCTION.**

Metal foam is a near-net or sponge-like shape cellular structure consisting of a solid matrix (also termed as skeletal configuration or struts), visual fascinating pores and pore openings. Porous metallic structures are generally classified into close-cell or open-cell interconnecting pores. The interconnecting pores or pore openings in porous metallic structures are generally considered as an open volume within the matrix network that allows the uniform length of passages and distribution. Understanding the behavior of fluid permeation through porous metallic structures is quite important in the design and optimization of enhanced porous materials for the process (Otaru 2018).

Porous media have a broad range of industrial application. Some researchers use idealized geometrical shapes to develop theoretical models for structure of porous media. Porous materials with a high range of porosities have been frequently used in many application because of its unique promising potentials, porous metals have become one of the most important material used in insulating transferring, storing and

dissipating thermal energy the benefits these characteristics confer have led to porous materials being widely used in practical applications such as thermal insulation, geothermal applications, cooling systems, heat exchangers in addition to chemical and nuclear engineering. Thus convective flow in porous materials have been investigated widely over recent decade and various aspect have been consider for different application so far (Wei zhong *et al.*,)

Porous metals possess a number of unique and and fascination, properties due to its relatively low density combined with some physical properties. Porous metal can be used as either a structural material or a functional material, or a combination of both structural and functional material. In recent years, a large number of porous metals base on different metallic materials, such as aluminum, copper, steel, magnesium, zinc and their alloys, have been exploited so far, several commercially available porous metals, such as porous aluminum, porus nickel and porous copper, have been used in engineering application (Xiaozhu 2013).



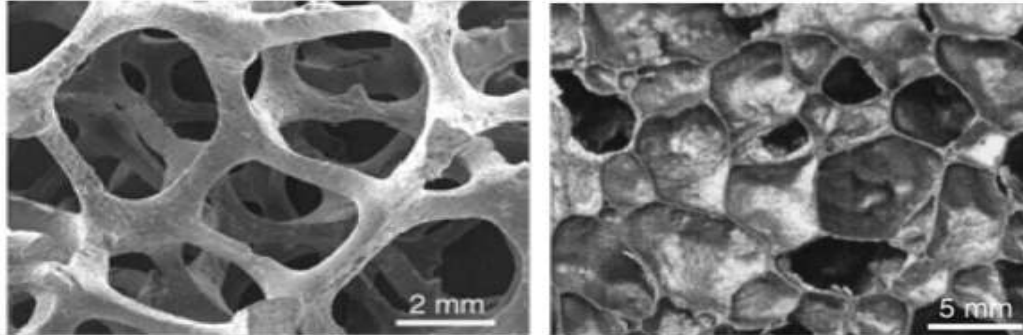
**Figure 1: Sample of a Porous metal.**

Porous metals attracted scientists attention in last century and are still receiving a growing interest in recent years due to their unique physical and structural properties (Ashby *et al.*, 2000)

### **Types of Porous Metal**

There are two types of porous metal: Closed-cell and Open-cell. The void in open-cell porous metals are interconnected, which provides pathways for fluid flow. The voids

in closed-cell porous metals on the other hand are not connected and are separated by the solid metal matrix. (J.M Baloyo 2016).



Open-cell porous metal

Closed-cell porous metal.

**Figure 2: Open-cell and close- cell porous metals.**

## **MATERIALS AND METHODS**

### **MATERIAL**

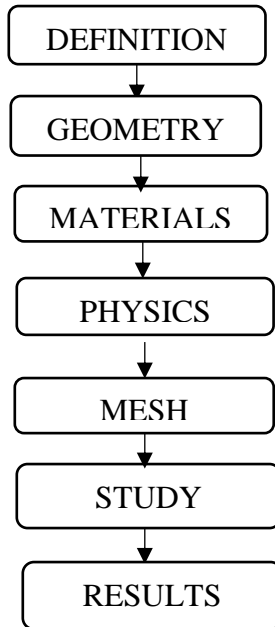
For this study, the following materials and equipment were used;

- Inconel 450 $\mu$ m
- Inconel 1200 $\mu$ m
- Recemat 1116 PPI
- Recemat 1723 PPI
- Porvair 7PPI
- The Comsol Multiphysics Software, Version 5.2
- Synopsys-Simpleware<sup>TM</sup> Software
- A Computer system (Folio 9470m EliteBookhp, Windows 10, 8GB RAM, 512 ROM, 2.40 GHz Processor Speed, 64-bit Operating System).

### **METHODOLOGY**

The methods employed in carrying out the 2D and 3D CFD modelling and simulation of five commercially available porous metallic structure and the dialation of samples with a focus on developement of airflow across these metals samples in the Darcy-Forchheimer-Turbulence regime. Computational fluid dynamics (CFD) simulation of air flow through these porous structures was performed by solving the steady – state compressible Stokes, Navier Stock and algebraic yPlus RANS turbulence model on a meshed fluid domain within a representative volume element(RVE), using the Single-Phase flow module in COMSOL Multiphysics 5.2. Meshing and mesh dependence study was also carried out on these samples in order to obtain an accurate and comprehensive information on the velocity and pressure gradients developed across

the porous structures as well as the permeability and form drag for each sample. The steps shown in the chart below were applied during the course of the CFD simulation and modelling:



The Navier-Stokes equation of flow in porous media is formed from the combination of the continuity equation and the momentum equation described below:

#### Continuity

$$0 = \nabla \cdot (\rho v) \quad (1.)$$

#### Creeping Flow

$$0 = \nabla \cdot \left[ P I + \mu (\nabla \cdot v + (\nabla \cdot v)^T) - \frac{2}{3} \mu (\nabla \cdot v) I \right] + F \quad (2.)$$

#### Navier-Stokes

$$\rho (v \cdot \nabla) v = \nabla \cdot \left[ P I + \mu (\nabla \cdot v + (\nabla \cdot v)^T) - \frac{2}{3} \mu (\nabla \cdot v) I \right] + F \quad (3.)$$

Where  $\mu$  is the dynamic viscosity of the fluid in kg/m.s;  $v$  is the velocity vector in m/s;  $\rho$  is fluid density in kg/m<sup>3</sup>;  $p$  is the pressure measured in Pa.

**Turbulent:** Algebraic yPlus RANS Turbulent models for slow moving fluid in the turbulent regime (Re 300-360)

$$\underbrace{\rho \frac{\partial v}{\partial t} + \rho(v \cdot \nabla)v}_{\text{Acceleration}} = \underbrace{\nabla \cdot [-p + (\mu + \mu_T)(\nabla v + (\nabla v)^T)] - \frac{2}{3} \nabla(\mu + \mu_T)(\nabla \cdot v)}_{\text{Force due to velocity gradient and pressure}} + \underbrace{F}_{\text{Force due external field}}$$

## RESULTS AND DISCUSSION

### RESULTS

**Table 1.** Pore-structure related and flow information of the “real” and “adapted” RCM-NCX 1116, Porvair 7PPI and Inconel 450 porous samples.

µCT Sample	Dp (mm)	Dw (mm)	ε (%)	L <sub>T</sub> (mm)	σ <sub>SB</sub> (mm <sup>-1</sup> )	σ <sub>ST</sub> (mm <sup>-1</sup> )	Viscous		Inertial	
							k <sub>0</sub> /10 <sup>-9</sup> m <sup>2</sup> Darcy	C (m <sup>-1</sup> )	C <sub>F</sub> [-]	
RCM-NCX 1116 [Real]	2.45	1.29	89.81	0.34	1.52	13.28	65.36	594.66	0.18	
RCM-NCX 1116 [DL1]	2.28	1.05	79.97	1.58	1.82	7.25	34.41	1420.19	0.22	
RCM-NCX 1116 [DL2]	1.98	0.89	71.64	1.70	2.27	5.73	20.83	2665.06	0.38	
RCM-NCX 1116 [DL3]	1.74	0.72	62.85	1.83	2.78	4.70	10.99	5369.88	0.37	
Porvair 7PPI [Real]	1.47	0.86	89.69	0.41	2.25	19.60	25.14	1105.67	0.23	
Porvair 7PPI [DL1]	1.43	0.80	85.83	1.48	2.38	14.45	19.96	1455.72	0.27	
Porvair 7PPI [DL2]	1.33	0.75	82.03	1.54	2.66	12.16	15.86	1894.16	0.31	
Porvair 7PPI [DL3]	1.23	0.71	78.05	1.61	3.00	10.66	12.10	2651.86	0.39	
Inconel 450µm [Real]	0.45	0.24	83.54	0.06	8.63	43.82	1.25	8541.55	0.34	
Inconel 450µm [DL1]	0.35	0.17	70.54	1.72	11.89	28.49	0.48	29190.67	0.64	
Inconel 450µm [DL2]	0.29	0.12	57.50	1.90	15.37	20.80	0.16	98884.37	1.22	

where DL1, DL2, and DL3 are symbols for the adapted-structures created by adding 1, 2 and 3 voxels to the skeletal phases of the materials respectively. Dp is the mean pore sizes (m), Dw is the mean pore openings (mm), ε is the porosity (%), L<sub>T</sub> is the strut or ligament thickness (mm), σ<sub>SB</sub> is the structure surface area per unit bulk volume (mm<sup>-1</sup>), σ<sub>ST</sub> is the structure surface area per unit structure volume (mm<sup>-2</sup>), k<sub>0</sub> is the Darcian permeability (m<sup>2</sup>), k<sub>f</sub> is the Forchheimer permeability (m<sup>3</sup>), C is the Form Drag (m<sup>-1</sup>) and C<sub>F</sub> is the Forchheimer coefficient [-].

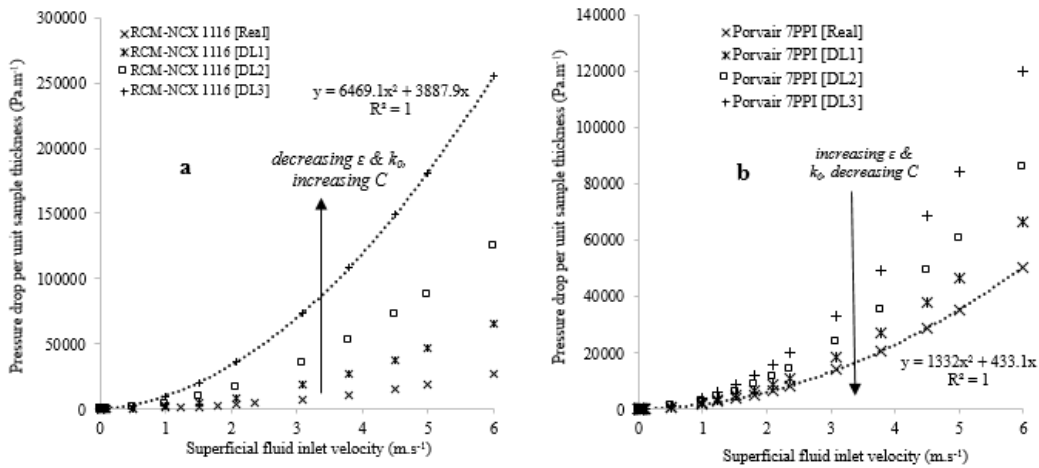


**Figure 1:** Plots of unit pressure drop [Pa.m<sup>-1</sup>] against superficial fluid inlet velocity (m.s<sup>-1</sup>) for fluid across real and structural adapted (a) Recemat RCM-NCX 1116 and (b) Porvair 7PPI porous samples

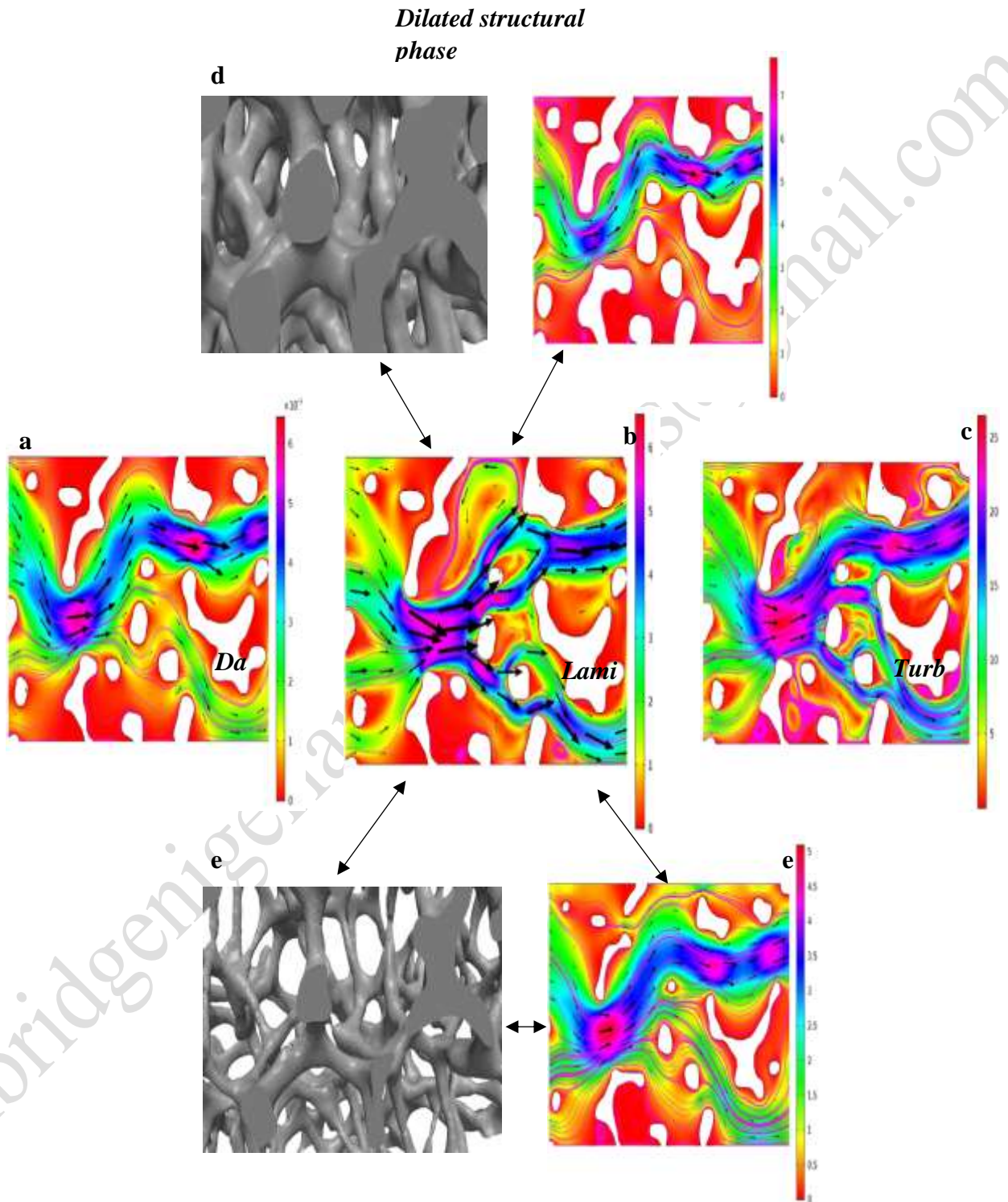


**Figure 2:** Fluid flow pattern at different regime

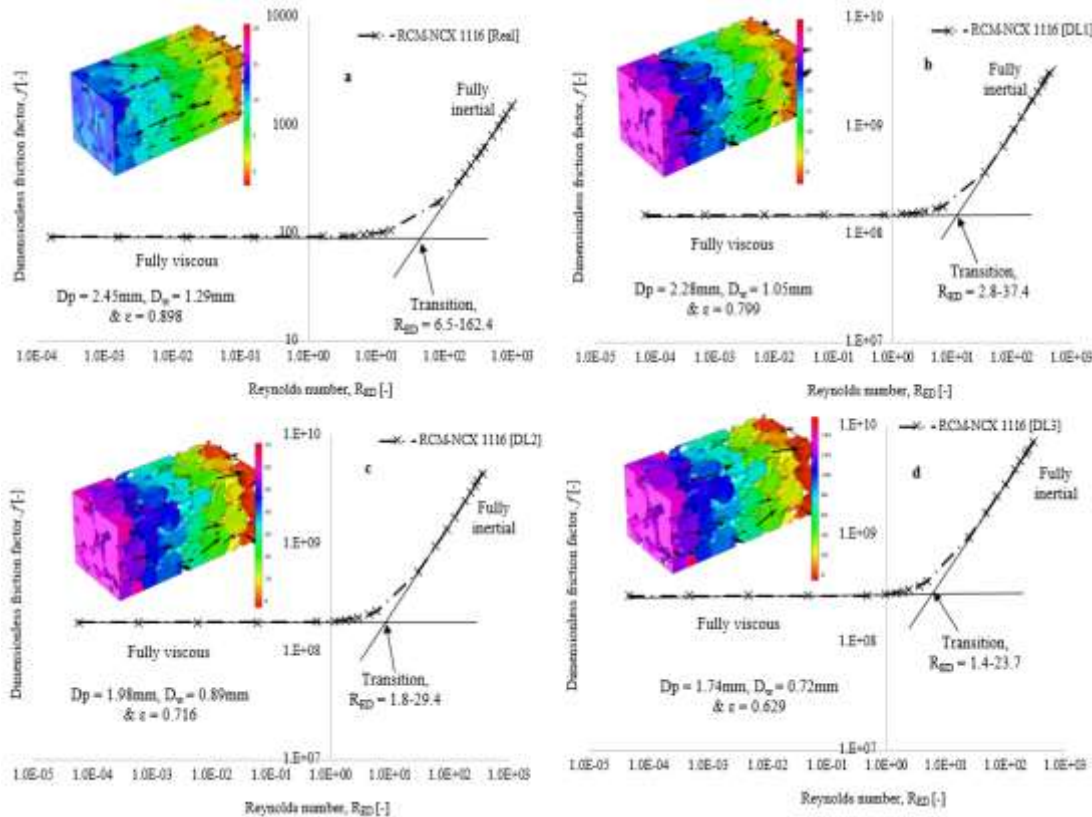


Figure 3: Representation of the fluid flow pattern for real and dilated recemat 1116 sample.

Samples	Porosity ( $\epsilon$ )	Ko $\times 10$ ( $m^2$ )	C ( $m^{-1}$ )
Inc 450 $\mu$ m(CFD)	0.84	1.601	8541.5
Inc 450 $\mu$ m(EXP) Oun and Kennedy 2015.	0.83	1.687	8530.7
Inc 1200 $\mu$ m(CFD)	0.906	22.639	11830.7
Inc 1200 $\mu$ m(EXP) Otaru et al 2019, Oun and Kennedy 2014.	0.900	21.66	1111.4

Figure 4: Validation table.

## CONCLUSION

The porosity of structural-adapted porous metals as shown from the table, the graphs and fluid flow pattern give better result as compared to that of real sample. The porosity(0.906) of the structural-adapted porous metals obtained is in agreement with that of the experimental work(0.900) therefore it can be concluded that computational fluid dynamics can be successfully use to investigate permeability and form drag and other related fluid flow behavior of porous metals.

## REFERENCES

- A.J. Otaru, H.P. Morvan, A.R. Kennedy, Modelling and optimisation of sound absorption in replicated microcellular metals. *Scripta Mater.* 150, 152–155 (2018)
- N. Dukhan, O. Bagci, M. Ozdemir, Experimental flow in various porous media and reconciliation of Forchheimer and Ergun relation. *Exp. Thermal Fluid Sci.* 57, 425–433 (2014)
- F. Garcia-Moreno, Commercial applications of metal foams: their properties and production. *Materials* 9, 85 (2016)
- P. Asholt, in *Metal Foams and Porous Metal Structures*, ed. by J. Banhart, M.F. Ashby, N.A. Fleck (MIT-Verlag, Bremen, 1999), p. 133
- V. Shapovalov, in *Porous and Cellular Materials for Structural Applications*, vol. 521, ed. by D.S. Schwartz et al. (MRS, Warrendale, 1998), p. 281
- M. Fink, O. Anderson, T. Seidel, A. Schlott, Strongly orthotropic open cell porous metal structures for heat transfer applications. *Metals* 8, 554 (2018)
- J. Banhart, Metal foams: production and stability. *Adv. Eng. Mater.* 8, 781–794 (2006)
- M. Bram, C. Stiller, H.P. Buchkremer, D. Stover, H. Bauer, Highporosity titanium, stainless steel and superalloy parts. *Adv. Eng. Mater.* 2, 196 (2000)
- A.J. Otaru, A.R. Kennedy, The permeability of virtual macroporous structures generated by sphere-packing models: comparison with analytical models. *Scripta Mater.* 124, 30–33 (2016)
- A.J. Otaru, H.P. Morvan, A.R. Kennedy, Measurement and simulation of pressure drop across replicated microcellular aluminium in the Darcy–Forchheimer regime. *Acta Mater.* 149, 265–275 (2018)
- A.J. Otaru, H.P. Morvan, A.R. Kennedy, Airflow measurement across negatively infiltration processed porous aluminium structures. *AIChE J.* (2019). <https://doi.org/10.1002/aic.16523>
- T.J. Lu, F. Chen, D. He, Sound absorption of cellular metals with semi-open cells. *J. Acoust. Soc. Am.* 108(4), 1697–1708 (2000)
- B.N. Asmar, P.A. Langston, A.J. Matchett, A generalized mixing index in discrete element method simulation of vibrated particulate beds. *Granul. Matter* 4(3), 129–138 (2002)
- A.J. Otaru, Fluid Flow and Acoustic Absorption in Porous metallic Structures Using Numerical Simulation and Experimentation, Ph.D. thesis, The University of Nottingham, United Kingdom (2018)
- H.K. Versteeg, W. Malasekara, An Introduction to Computational Fluid Dynamics—The Finite Volume Method, 2nd edn. (Pearson Education Limited, London, 2007)
- D.A. Nield, A. Bejan, *Convection in Porous Media*, 2nd edn. (Springer, New York, 1992), pp. 8–91
- G.A. Narsilio, O. Buzzi, S. Fityus, T.S. Yun, D.W. Smith, Upscaling of Navier–Stokes equation in porous media: theoretical, numerical and experimental approach. *Comput. Geotech.* 36, 1200–1206 (2009)
- T.P. De Carvalho, H.P. Morvan, D. Hargreaves, H. Oun, A. Kennedy, Pore-scale numerical investigation of pressure drop behaviour across open-cell metal foams. *Transp. Porous Media* 117(2), 311–336 (2017)
- H. Darcy, *Les Fontaines Publiques de la Ville de Dijon* (Dalmont, Paris, 1856) 53. Comsol, Introduction to the Acoustic Module, US Patent, 7, 519, 518; 7, 596, 474 and 7, 623, 991 (2015)
- M. Piatek, A. Gancarczyk, M. Iwaniszyn, P.J. Jodlowski, J. Lojewska, A. Kolodziej, Gas-phase flow resistance of metal foams: experiments and modelling. *AIChE J.* 63(6), 1799–1803 (2017)
- J.L. Lage, P.S. Krueger, A. Narasimham, Protocol for measuring permeability and form coefficient of porous media. *Phys. Fluids* 17, 088101 (2005)
- Dukhan, C.A. Minjeur, A two-permeability approach for assessing flow properties in cellular metals. *J. Porous Mater.* 18(2), 417–424 (2010)
- B. Antohe, J.L. Lage, D.C. Price, R.M. Weber, Experimental determination of the permeability and inertial coefficients of mechanically compressed aluminium metal layers. *ASME J. Fluids Eng.* 11, 404–412 (1997)
- H. Oun, A.R. Kennedy, Experimental investigation of pressure drop characterization across multilayer porous metal structure. *J. Porous Mater.* 21, 1133–1141 (2014)
- J.F. Despois, A. Mortensen, Permeability of open-pore microcellular materials. *Acta Mater.* 53, 1381–1388 (2005)
- A.J. Otaru, Enhancing the sound absorption performance of porous metals using tomography images. *Appl. Acoust.* 140, 183–189 (2019)
- Y. Champoux, M.R. Stinson, On acoustical models for sound propagation in rigid frame porous materials and the influence of shape factors. *J. Acoust. Soc. Am.* 92(2), 1120–1131 (1992)